Comparison of CZT SPECT and conventional SPECT for assessment of contractile function, mechanical synchrony and myocardial scar in patients with heart failure

Dayong Wu, MD,[a,b] Zongyao Zhang, BSc,[a] Rongzheng Ma, MD,[a] Feng Guo, BSc,[a] Lei Wang, MD, PhD,[a] and Wei Fang, MD[a]

[a] Department of Nuclear Medicine, Fuwai Hospital, National Center for Cardiovascular Diseases, Chinese Academy of Medical Sciences and Peking Union Medical College, Beijing, China
[b] Department of Nuclear Medicine, Hebei General Hospital, Shijiazhuang, Hebei, China

Received Mar 1, 2017; accepted May 31, 2017
doi:10.1007/s12350-017-0952-6

Aim. **The aim of this study was to compare CZT-SPECT (CZT SPECT) to conventional SPECT (C-SPECT) in the assessment of left ventricular myocardial scar, contractile function, and mechanical synchrony in patients with heart failure (HF).**

Methods. **Fifty-nine patients with HF who were referred for myocardial perfusion/metabolism imaging were enrolled. All patients underwent resting ^{99m}Tc-MIBI gated myocardial perfusion imaging using a CZT SPECT camera and a C-SPECT camera, respectively, and ^{18}F-FDG PET myocardial metabolism imaging within three days. Summed rest score (SRS) and total perfusion defect (TPD) (as indices of perfusion abnormality), left ventricular (LV), end diastolic volume (EDV), end systolic volume (ESV), and ejection fraction (EF) (as indices of LV systolic function), and histogram band width (BW) and standard deviation (SD) (as indices of mechanical synchrony) were analyzed by automated software while the perfusion/metabolism patterns were analyzed visually.**

Results. **There was a good correlation between CZT SPECT and C-SPECT for SRS and TPD. CZT SPECT tended to underestimate SRS and TPD compared to C-SPECT. CZT-SPECT and C-SPECT showed excellent agreement in assessing the perfusion/metabolism pattern though a small proportion of normal segments (6.6%) identified by CZT/PET exhibited mismatch pattern on C-SPECT/PET. CZT SPECT also showed excellent correlation with C-SPECT in measuring EDV, ESV, and EF. Finally, BW and SD measured by CZT SPECT correlated well with C-SPECT but CZT SPECT tended to overestimate BW and SD compared to C-SPECT.**

Conclusion. **CZT SPECT provided comparable data to C-SPECT for measuring LV scar, function and synchrony at a considerable reduction in imaging time. CZT SPECT holds a promise for comprehensive evaluation of myocardial performance in patients with HF. (J Nucl Cardiol 2019;26:443–52.)**

Key Words: SPECT • CZT • left ventricular function • mechanical synchrony • myocardial scar • heart failure

Electronic supplementary material The online version of this article (doi:10.1007/s12350-017-0952-6) contains supplementary material, which is available to authorized users.

The authors of this article have provided a PowerPoint file, available for download at SpringerLink, which summarises the contents of the paper and is free for re-use at meetings and presentations. Search for the article DOI on SpringerLink.com.

Reprint requests: Lei Wang, MD, PhD, and Wei Fang, MD, Department of Nuclear Medicine, Fuwai Hospital, National Center for Cardiovascular Diseases, Chinese Academy of Medical Sciences and Peking Union Medical College, Beijing, China; *leiwangfw@126.com* and *nuclearfw@126.com*

1071-3581/$34.00

Abbreviations

CZT SPECT	Cadmium-zinc-telluride-based SPECT
C-SPECT	Conventional SPECT
HF	Heart failure
SRS	Summed rest score
TPD	Total perfusion defect
EDV	End diastolic volume
ESV	End systolic volume
BW	Band width
SD	Standard deviation
MPI	Myocardial perfusion imaging

See related editorial, pp. 453–455

INTRODUCTION

Comprehensive evaluation of myocardial performance including myocardial scar burden and left ventricular (LV) contractile function and mechanical synchrony is important in patients with heart failure (HF) to assess disease severity, therapeutic options, and clinical outcome including the appropriateness of coronary revascularization and cardiac resynchronization therapy (CRT).[1–4] ^{99m}Tc-MIBI SPECT myocardial perfusion imaging (MPI) and ^{18}F-FDG PET have been extensively used to address these issues.

Two dedicated cameras with semiconductor cadmium-zinc-telluride (CZT) detectors have been commercially available recently. Compared with conventional Anger cameras, either D-SPECT (Spectrum Dynamics, Biosensors, Israel) with a parallel-hole collimation or Discovery NM530c camera (GE Healthcare, Haifa, Israel) with a multi-pinhole collimation exhibits higher spatial resolution and enhanced photon sensitivity.[5–7] Additionally, due to its design of heart-centric method of collimation, CZT-based SPECT (CZT SPECT) has been increasingly used in recent years. Data suggest that CZT SPECT cameras are able to yield images with excellent quality despite reduced acquisition time and/or administered radiotracer activity dose to patients.[8,9]

MPI acquired by CZT SPECT has been compared to that from conventional SPECT (C-SPECT), suggesting a high diagnostic accuracy for detecting global and regional ischemia and for measuring LV volumes and ejection fraction (EF) and mechanical dyssynchrony.[10–14] However, the performance of CZT SPECT specifically in HF patients to address above-mentioned measurements has not been done.

The purpose of this study therefore was to compare the performance of CZT SPECT to C-SPECT and to PET metabolic imaging in a cohort of patients with HF.

METHODS

Study Population

From July 2016 to October 2016, a total of 75 patients with HF who were referred for MPI and metabolism imaging were initially enrolled at Fuwai Hospital. The diagnosis of HF was made according to the guidelines for the diagnosis and treatment of acute and chronic HF.[15] We excluded 16 patients with atrial fibrillation and thus the remaining 59 patients constituted the study group. All patients underwent resting ^{99m}Tc-MIBI gated MPI using CZT SPECT and C-SPECT, respectively, followed by ^{18}F-FDG PET imaging within three days. The study was approved by the local institution's ethics committee of Fuwai Hospital. All subjects signed informed consent forms.

Acquisition and Reconstruction of CZT SPECT and C-SPECT Imaging

Patients underwent resting gated MPI with C-SPECT (Symbia T16, Siemens) at 60 min after the injection of ^{99m}Tc-MIBI (740 MBq). Immediately after gated MPI with C-SPECT was completed, gated MPI with CZT SPECT (DSPECT, Spectrum Dynamics) was obtained. Acquisition time for C-SPECT was 12 min and for CZT SPECT 3 min.

C-SPECT camera was equipped with a low-energy, high-resolution collimation. C-SPECT gated MPI was performed with 32 steps (20 s/projection) over a 90° orbit per detector for a total of 64 projections using a 64 × 64 matrix, a zoom factor of 1.78 and an energy window centered on the photopeak of 140 keV ± 10%. During each step of scanning, the two detectors were close to the patient chest using body-contour acquisition mode. Perfusion images of C-SPECT were reconstructed with ordered subsets expectation maximization (OSEM) (2 iterations and 8 subsets) with a post Gaussian filter (full width at half maximum, 10 mm) using the vender recommended image reconstruction protocol without additional resolution recovery. Gated images of C-SPECT were reconstructed using filtered back-projection with a Butterworth filter (cutoff, .5; order, 5).

The CZT SPECT camera comprises nine rotating pixelated detector columns of CZT crystals. Each detector is equipped with a wide-angle square-hole tungsten collimator. During scanning, each detector rotated around its central axis focusing on the region of interest drawn on an image from a preliminary scan. Perfusion and gated images of CZT SPECT were reconstructed using an algorithm of 3-dimensional iterative reconstruction (7 iterations and 32 subsets) to compensate for collimator-related loss in spatial resolution provided by the manufacturer.[5,16]

Acquisition and Reconstruction of PET Imaging

Patients fasted for at least 8 h, then they were given a 20-50 g oral glucose load or a regular short-acting insulin

intravenous injection according to the serum glucose level.[17] Gated PET imaging (Truepoint Biography 64, Siemens Healthcare) was performed for 10 min (8 frames/cardiac cycle, 3-dimensional mode) at 60 min after injection of ^{18}F-FDG (185 MBq). Images were reconstructed by attenuation weighted-OSEM iterative algorithm (4 iterations, 8 subsets, matrix: 128 × 128, zoom:2.0).

Imaging analysis. All MPI images obtained by CZT SPECT or C-SPECT camera were analyzed by QPS software (Cedars-Sinai Medical Center) to obtain the summed rest score (SRS) and total perfusion defect (TPD). SRS is based on a 17-segment model of LV and a 5-point scale to assess the extent and severity of perfusion abnormality. TPD, another index for the extent and severity of perfusion abnormality, is based on a comparison against a database of normal subjects and expressed as a percentage of the LV myocardium.[18] Manual correction was performed in the case of inadequate automatic delineation.

MPI images acquired by CZT SPECT or C-SPECT camera were compared with ^{18}F-FDG PET images. Images were analyzed and interpreted by two experienced nuclear cardiologists independently. The horizontal long-axis and vertical long-axis slices of images were shown on the QPS platform. The17-segment model was used.[19]

^{99m}Tc-MIBI and ^{18}F-FDG uptakes in all segments were scored with a semi-quantitative 4-grade scoring system (0, normal; 1, mild; 2, moderate; 3, severe reduction of radioisotope uptake). The segments were divided into 4 groups with different patterns of perfusion/metabolism.

Group 1 (normal perfusion/metabolism) consisted of segments with normal ^{99m}Tc-MIBI (score 0) and normal ^{18}F-FDG (score 0) uptake. Group 2 (perfusion/metabolism mismatch) consisted of segments with reduced ^{99m}Tc-MIBI uptake (score 1, 2, or 3) and preserved/relatively increased ^{18}F-FDG uptake (^{18}F-FDG score < ^{99m}Tc-MIBI score). Group 3 (mild perfusion/metabolism match) consisted of segments with a mild reduction in ^{99m}Tc-MIBI uptake (score 1) and a concordant mild reduction in ^{18}F-FDG uptake (score 1). Group 4 (moderate perfusion/metabolism match) consisted of segments with a moderate reduction in ^{99m}Tc-MIBI uptake (score 2) and a concordant moderate reduction in ^{18}F-FDG uptake (score 2). Group 5 (severe perfusion/metabolism match) consisted of segments with a severe reduction in ^{99m}Tc-MIBI uptake (score 3) and a concordant severe reduction in ^{18}F-FDG uptake (score 3).[20]

QGS software (Cedars-Sinai Medical Center) was used to compute LVEF, end diastolic volume (EDV), and end systolic volume (ESV) as well as mechanical synchrony using phase analysis to derive histogram band width (BW) and standard deviation (SD).

Statistical Analysis

Continuous variables were expressed as mean ± SD or median (interquartile range) and categorical variables were expressed as percentage or numbers. Differences between parameters obtained from two devices were compared with a paired *t* test (2-tailed). Correlation between devices was evaluated using the Pearson correlation. Agreement of continuous data between devices was assessed by the concordance correlation coefficient (CCC) and the Bland–Altman analysis. Agreement of categorical data was assessed by Kappa statistic. Statistical significance was assessed at a $P < .05$ (2-tailed). All statistical analyses were performed using MedCalc 15.2.2 software.

RESULTS

Patient Characteristics

Clinical characteristics of all patients are shown in Table 1.

There was good correlation between CZT SPECT and C-SPECT for SRS and TPD (SRS, $r = .92$, $P < .0001$; TPD, $r = .94$, $P < .0001$, Figure 1A, C). Agreement between CZT SPECT and C-SPECT for SRS and TPD was good (SRS, CCC = .90, 95% CI .83-.94; TPD, CCC = .93, 95% CI .88-.96).CZT SPECT tended to underestimate SRS and TPD compared to C-SPECT (mean bias, SRS: −2.7, TPD: −2.5%; 95% limits of agreement, SRS: −11.6-6.2, TPD: −14.2%-9.2%; Figure 1B, D), but there was no statistically significant difference (SRS, 18.0 ± 11.5 vs. 20.7 ± 11.3, $P = .202$; TPD, 26.2% ± 17.3% vs. 28.7% ± 16.3%, $P = .425$).

CZT-SPECT and C-SPECT showed excellent agreement in determining the perfusion/metabolism pattern (Kappa value = .85, $P < .0001$, Table 2). Of the total 1003 segments, CZT SPECT/PET detected 117 segments with severe match, 38 with moderate match, and 74 with mild match patterns, while C-SPECT/PET detected 120 segments with severe match, 40 with moderate match, and 61 with mild match patterns. Slight difference existed in the mismatch and normal segments distribution. In the 575 normal segments detected by CZT SPECT/PET, 6.6% (38/575) demonstrated mismatch on C-SPECT/PET. A representative image of this different interpretation is shown in Figure 2A.

Value of measuring LV contractile function. The mean values of EDV, ESV, and EF measured by CZT SPECT and C-SPECT are shown in Table 3. EDV, ESV, and LVEF measured by CZT SPECT correlated well with these parameters measured by C-SPECT (EDV, $r = .98$, $P < .0001$; ESV, $r = .98$, $P < .0001$; LVEF, $r = .91$, $P < .0001$) (Figure 3A, C, E). CCC and Bland–Altman analyses showed that the agreement of EDV, ESV, EF between CZT SPECT and C-SPECT was good (EDV, CCC = .98, 95% CI .96-.98, mean bias: 4.3 mL, limits of agreement: −28.3 mL-36.8 mL; ESV, CCC = .98, 95% CI .97-.99, mean bias: 2.3 mL, limits of agreement: −25.7-30.3 mL; LVEF, CCC = .91, 95% CI .86-.95, mean bias: .2%, limits of agreement: −7.7%-8.1%) (Figure 3B, D, F).

Table 1. Clinical characteristics

Parameter	
Gender [male (%)]	49 (83.1)
Age (years)	54.2 ± 13.1
Blood pressure (mmHg)	
Systolic	120 (16.8)
Diastolic	74.3 ± 8.7
Heart rate (bpm)	73.8 ± 9.1
NYHA heart failure functional class [*n* (%)]	
I	10 (16.9)
II	21 (35.6)
III	26 (44.1)
IV	2 (3.4)
Diagnosis [n (%)]	
Coronary artery disease	46(78.0)
Dilated cardiomyopathy	9 (15.3)
Congenital heart disease	2 (3.4)
Hypertrophic cardiomyopathy	2 (3.4)
History [*n* (%)]	
Myocardial infarction	42 (71.2)
Ventricular aneurysm	14 (23.7)
Prior PCI	11 (18.6)
Hypertension	29 (49.2)
Hyperlipidemia	34 (57.6)
Smoking	20 (33.9)
Alcoholic	3 (5.1)
LBBB	4 (6.8)
RBBB	1 (1.7)
Medications [*n* (%)]	
Anticoagulant	47 (79.7)
Diuretics	50 (84.7)
Calcium channel blocker	45 (76.3)
Beta-blocker	53 (89.8)
ACE inhibitors	29 (49.2)
Nitrates	47 (79.7)
Echocardiography LVEF(%)	36.2 ± 6.5
NTPro-BNP (pg/mL)	1145 (1715.1)

NYHA, New York Heart Association; *PCI*, percutaneous coronary intervention; *LBBB*, left bundle branch block; *RBBB*, right bundle branch block; *ACE*, angiotensin converting enzyme; *LVEF*, left ventricular ejection fraction; *NTPro-BNP*, N-terminal pro-brain natriuretic peptide

LV Mechanical Dyssynchrony

The mean values of BW and SD measured by CZT SPECT and C-SPECT are shown in Table 3.BW, and SD measured by CZT SPECT had good correlations with those from C-SPECT (BW, $r = .84$, $P < .0001$; SD, $r = .82$, $P < .0001$) (Figure 4A, C). The agreement between CZT SPECT and C-SPECT was good for BW measurement (CCC = .82, 95% CI, .72-.88), but was moderate for SD (CCC = .74, 95% CI .62-.83). Compared to C-SPECT, CZT SPECT overestimated SD (mean bias: 6.5°; 95% limits of agreement: −14.5°-27.5°; Figure 4D) ($P < .05$; Table 2). A trend of overestimation of BW was shown (mean bias: 11.6°, limits of agreement: −48.5°-71.8°; Figure 4B), but the difference was not statistically significant ($P > .05$; Table 3). Representative images of phase analysis from two modalities are shown in Figure 2B.

DISCUSSION

The present study is the first to examine the role of CZT SPECT in patients with HF. Our data showed that CZT SPECT with a short acquisition time (3 min) provided comparable results to C-SPECT (with 4 times longer acquisition time) for measuring important indices of LV performance including scar burden, EF, EDV, ESV, and mechanical dyssynchrony. These data compliment other data showing the value of CZT SPECT MPI in detecting myocardial ischemia.[21,22]

The utility of ^{99m}Tc-MIBI C-SPECT and ^{18}F-FDG PET imaging has been widely explored in HF to assess the myocardial scar and viability as viable and scarred myocardium have distinctly different match or mismatch patterns, which may determine the best option of therapy and clinical outcomes.[4,20]

In the current study, combined CZT SPECT MPI/PET imaging showed comparable diagnostic confidence to similar data obtained by C-SPECT MPI/PET although CZT SPECT/PET detected relatively more normal myocardial segments, while these segments demonstrated mismatch pattern on the conventional imaging, consistent with the relatively lower perfusion abnormality score found in the CZT SPECT MPI. Possible explanation for the discordance is the low spatial resolution and radionuclide counts per pixel on C-SPECT imaging.[5–7] Due to partial volume effect, the counts per pixel are underestimated. With much higher spatial resolution (2 times fold over the traditional device),[23] CZT SPECT may be able to distinguish mild perfusion defects from normal segments. We also noticed that images of C-SPECT were easily to be affected by artifacts from diaphragm and intestinal uptake due to limited spatial resolution, while CZT SPECT of a better image quality.[24,25]

Our results in assessing LV function and synchrony are in agreement of Giorgetti et al. and Cochet et al. in patients with known or suspected coronary artery disease.[26,27] Both results suggested that CZT SPECT was able to accurately quantify LVEF with no significant difference compared to cardiac MRI but underestimated LV volumes. Data from our study showed that CZT SPECT agreed well with C-SPECT

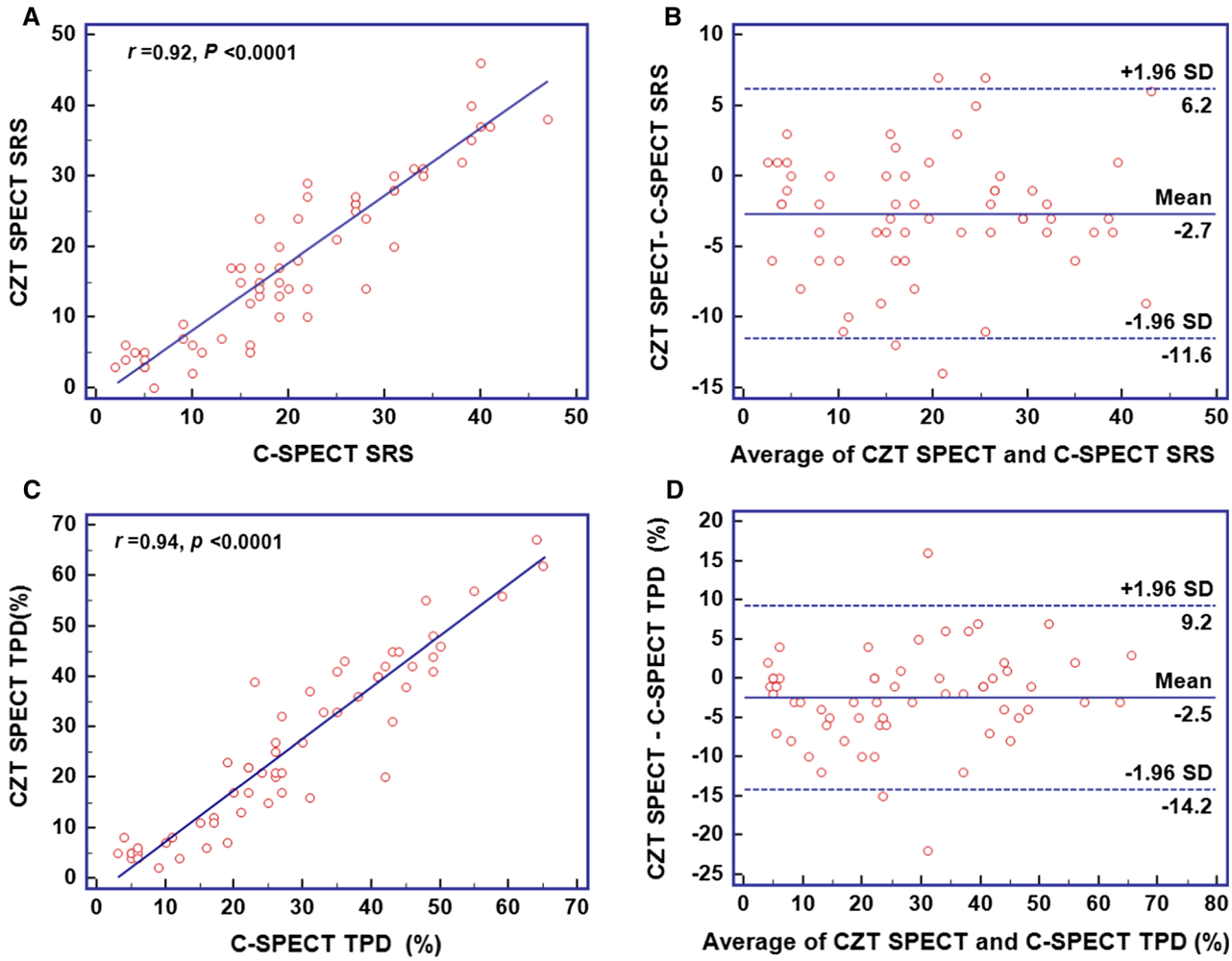

Figure 1. Correlation between CZT SPECT and C-SPECT for measurement of SRS (**A**) and TPD (**C**) and Bland–Altman plots for SRS (**B**) and TPD (**D**).

Table 2. Comparison of myocardial perfusion/metabolism pattern between CZT SPECT/PET and C-SPECT/PET

	CZT SPECT/PET*					
C-SPECT/PET*	**Normal**	**Mismatch**	**Mild Match**	**Moderate Match**	**Severe Match**	**Total**
Normal	523	5	4	0	0	532
Mismatch	38	191	17	2	2	250
Mild match	14	1	46	0	0	61
Moderate match	0	1	7	32	0	40
Severe match	0	1	0	4	115	120
Total	575	199	74	38	117	1003

* Kappa value is .85 ($P < .0001$)

in estimating EF, EDV, and ESV suggesting that CZT SPECT could also be used in patients with HF with worse LV function.

Patients with HF frequently present LV dyssynchrony, and may be candidates for CRT; but a considerable proportion of such patients may not

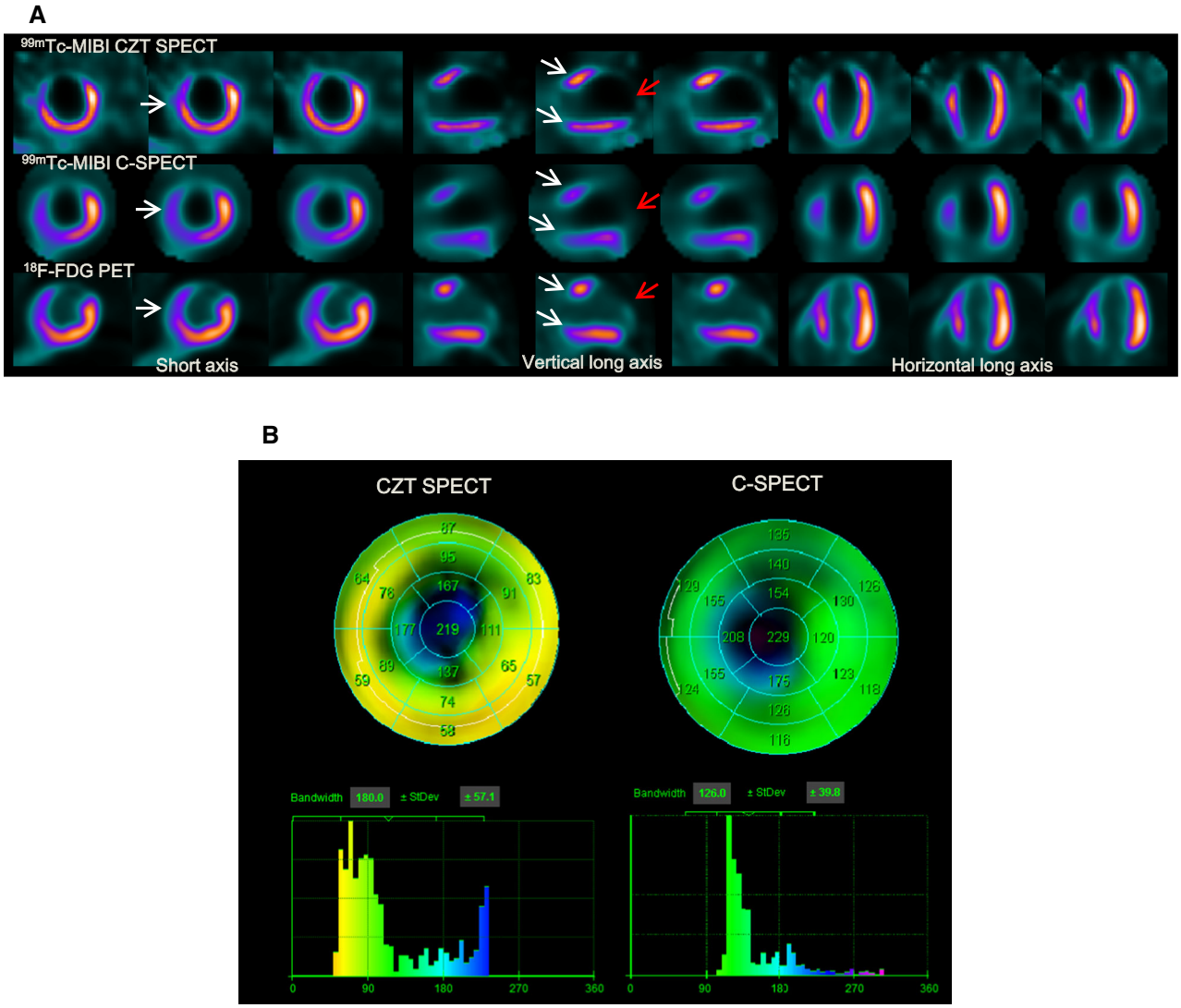

Figure 2. Representative images of perfusion/metabolism (**A**) and phase analysis (**B**) from a heart failure patient (male, 57 years, LVEF = 25%) with myocardial infarction and apical ventricular aneurysm. (**A**) The inferior, anterior basal, and septal segments (*white arrows*) were defined as normal by CZT SPECT/PET, but as perfusion/metabolism mismatch by C-SPECT/PET. The apex, anterior apical and anterior mid segments demonstrated severe match pattern (*red arrows*) on both CZT SPECT/PET and C-SPECT/PET. (**B**) BW measured by CZT SPECT and C-SPECT are 180° and 126°, respectively. SD measured by CZT SPECT and C-SPECT are 57.1° and 39.8°.

Table 3. Comparison of EDV, ESV, and LVEF between CZT and C-SPECT

	CZT SPECT	C-SPECT	*t*	*P value*
EDV (mL)	206.6 ± 80.3	202.3 ± 78.3	−.293	.770
ESV (mL)	155.0 ± 75.3	152.6 ± 74.4	−.169	.867
LVEF (%)	27.7 ± 9.6	27.4 ± 9.8	−.133	.895
BW(°)	141.2 ± 57.2	129.6 ± 49.7	−1.180	.240
SD (°)	41.6 ± 18.5	35.1 ± 14.8	−2.114	.037

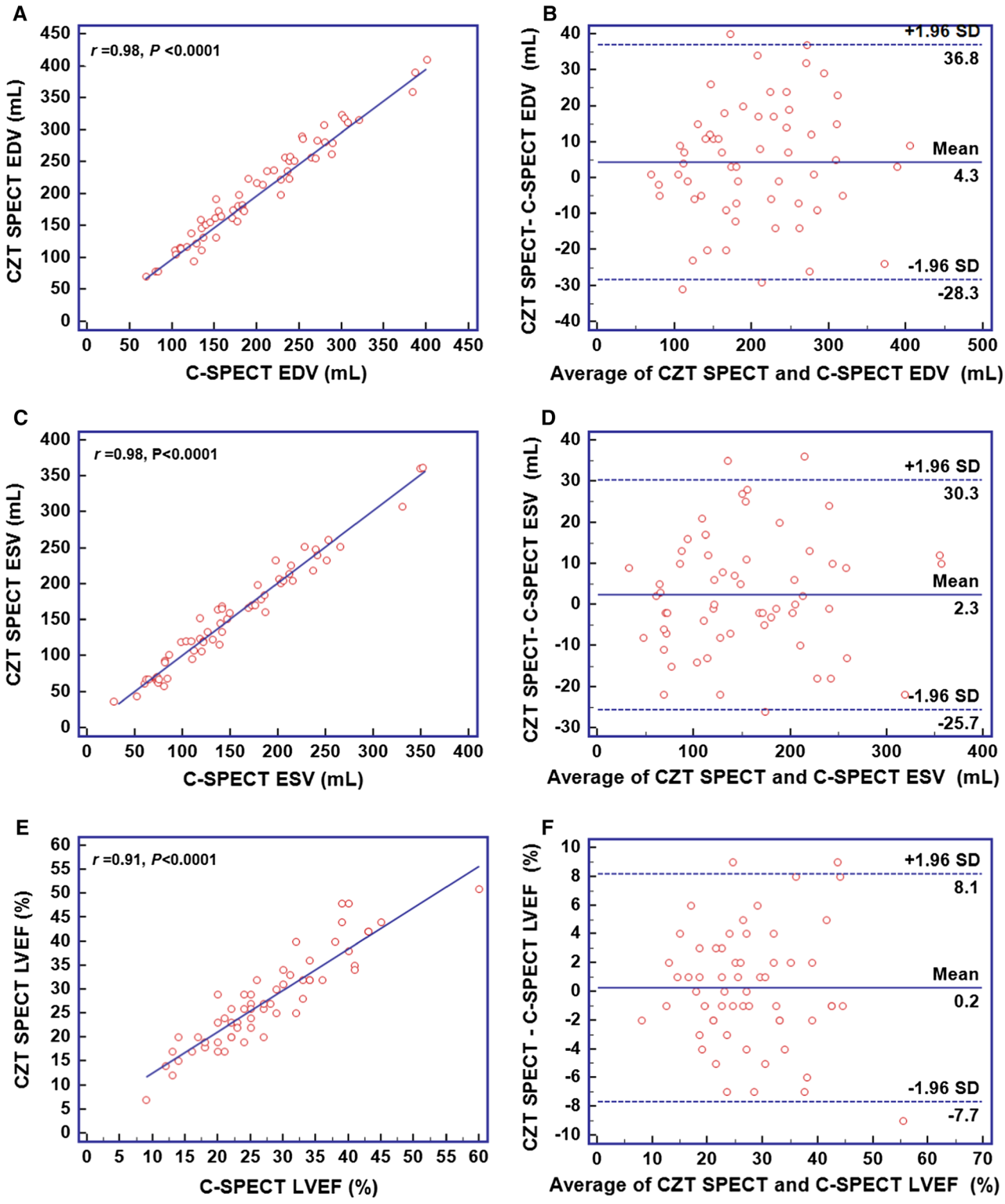

Figure 3. Correlations and Bland–Altman plots between CZT SPECT and C-SPECT for measurement of EDV (**A**, **B**), ESV (**C**, **D**) and LVEF (**E**, **F**).

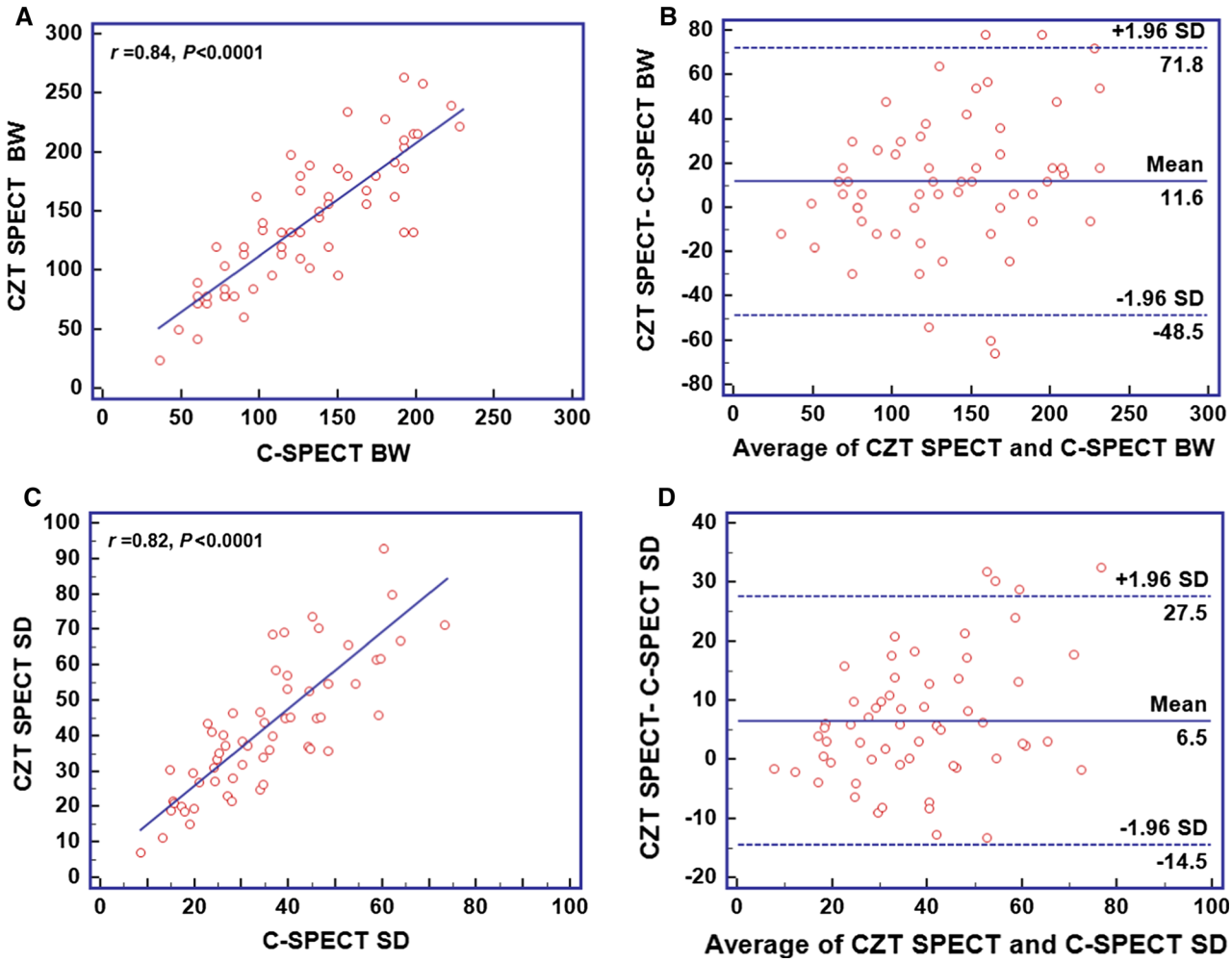

Figure 4. Correlations and Bland–Altman plots between CZT SPECT and C-SPECT for measurement of BW (**A**, **B**) and SD (**C**, **D**).

respond well to CRT.[28,29] MPI could be used to assist in the selection of candidates of CRT.[30,31] BW > 135° or SD > 43° acquired by phase analysis from gated SPECT MPI have been shown to predict responders to CRT with sensitivity and specificity ∼70%.[32]

Few studies have reported on the application of CZT SPECT in phase analysis. Pazhenkottil and coworkers demonstrated that normal BW and SD obtained with a CZT SPECT camera (35.9 ± 7.7°, 12.6 ± 3.5°) were comparable with a C-SPECT camera (34.8 ± 6.6°, 11.1 ± 2.1°, $P > .05$).[12] Similarly, our data showed that there were excellent correlations between BW and SD acquired by CZT SPECT and C-SPECT, but C-SPECT tended to underestimate slightly BW and SD (P = NS) in our patients with HF. As the method of phase analysis to assess synchrony from Fourier transform depends on relative change in myocardial count density instead of the magnitude of count density in a voxel over a cardiac cycle, it is therefore measurement of BW and SD may not be affected among gated SPECT images with different image resolutions. As demonstrated by our study, CZT SPECT provided comparable images for assessment of synchrony to C-SPECT.

LIMITATIONS

A limitation of this study is that follow-up of these patients was not performed, so the outcome of the segments with different patterns on CZT SPECT/PET and C-SPECT/PET is not known. Whether CZT SPECT/PET would add more information in differentiation of normal myocardium from mild ischemia for HF patients remains to be determined.

NEW KNOWLEDGE GAINED

This study compared the use of CZT SPECT to C-SPECT in patients with HF. CZT SPECT provided comparable information for assessment of LV perfusion, scar, function, and synchrony to C-SPECT at a shorter acquisition time.

CONCLUSION

Our results demonstrate that with a significant reduction in scan times, CZT SPECT holds promise for comprehensive evaluation of myocardial performance in patients with HF.

Disclosure

The authors declare that they have no conflict of interest.

References

1. Morishima I, Okumura K, Tsuboi H, Morita Y, Takagi K, Yoshida R, et al. Impact of basal inferolateral scar burden determined by automatic analysis of ^{99}mTc-MIBI myocardial perfusion SPECT on the long-term prognosis of cardiac resynchronization therapy. Europace 2017;19:573–80.
2. Juneau D, Erthal F, Chow BJ, Redpath C, Ruddy TD, Knuuti J, et al. The role of nuclear cardiac imaging in risk stratification of sudden cardiac death. J Nucl Cardiol 2016;23:1380–98.
3. Nudi F, Di Belardino N, Versaci F, Pinto A, Procaccini E, Neri G, et al. Impact of coronary revascularization vs medical therapy on ischemia among stable patients with or suspected coronary artery disease undergoing serial myocardial perfusion scintigraphy. J Nucl Cardiol 2016. doi:10.1007/s12350-016-0504-5.
4. Lehtinen M, Schildt J, Ahonen A, Nikkinen P, Lauerma K, Sinisalo J, et al. Combining FDG-PET and ^{99}mTc-SPECT to predict functional outcome after coronary artery bypass surgery. Eur Heart J Cardiovasc Imaging 2015;16:1023–30.
5. Imbert L, Poussier S, Franken PR, Songy B, Verger A, Morel O, et al. Compared performance of high-sensitivity cameras dedicated to myocardial perfusion SPECT: A comprehensive analysis of phantom and human images. J Nucl Med 2012;53:1897–903.
6. Takahashi Y, Miyagawa M, Nishiyama Y, Ishimura H, Mochizuki T. Performance of a semiconductor SPECT system: Comparison with a conventional Anger-type SPECT instrument. Ann Nucl Med 2013;27:11–6.
7. Songy B, Lussato D, Guernou M, Queneau M, Geronazzo R. Comparison of myocardial perfusion imaging using thallium-201 between a new cadmium-zinc-telluride cardiac camera and a conventional SPECT camera. Clin Nucl Med 2011;36:776–80.
8. Herzog BA, Buechel RR, Katz R, Brueckner M, Husmann L, Burger IA, et al. Nuclear myocardial perfusion imaging with a cadmium-zinc-telluride detector technique: optimized protocol for scan time reduction. J Nucl Med 2010;51:46–51.
9. Nakazato R, Berman DS, Hayes SW, Fish M, Padgett R, Xu Y, et al. Myocardial perfusion imaging with a solid-state camera: Simulation of a very low dose imaging protocol. J Nucl Med 2013;54:373–9.
10. Buechel RR, Herzog BA, Husmann L, Burger IA, Pazhenkottil AP, Treyer V, et al. Ultrafast nuclear myocardial perfusion imaging on a new gamma camera with semiconductor detector technique: First clinical validation. Eur J Nucl Med Mol Imaging 2010;37:773–8.
11. Esteves FP, Raggi P, Folks RD, Keidar Z, Askew JW, Rispler S, et al. Novel solid-state-detector dedicated cardiac camera for fast myocardial perfusion imaging: Multicenter comparison with standard dual detector cameras. J Nucl Cardiol 2009;16:927–34.
12. Gimelli A, Bottai M, Giorgetti A, Genovesi D, Kusch A, Ripoli A, et al. Comparison between ultrafast and standard single-photon emission CT in patients with coronary artery disease: A pilot study. Circ Cardiovasc Imaging 2011;4:51–8.
13. Pazhenkottil AP, Buechel RR, Herzog BA, Nkoulou RN, Valenta I, Fehlmann U, et al. Ultrafast assessment of left ventricular dyssynchrony from nuclear myocardial perfusion imaging on a new high-speed gamma camera. Eur J Nucl Med Mol Imaging 2010;37:2086–92.
14. Bailliez A, Lairez O, Merlin C, Piriou N, Legallois D, Blaire T, et al. Left ventricular function assessment using 2 different cadmium-zinc-telluride cameras compared with a gamma-camera with cardiofocal collimators: dynamic cardiac phantom study and clinical validation. J Nucl Med 2016;57:1370–5.
15. Ponikowski P, Voors AA, Anker SD, Bueno H, Cleland JG, Coats AJ, et al. 2016 ESC Guidelines for the diagnosis and treatment of acute and chronic heart failure: The Task Force for the diagnosis and treatment of acute and chronic heart failure of the European Society of Cardiology (ESC)Developed with the special contribution of the Heart Failure Association (HFA) of the ESC. Eur Heart J 2016;37:2129–200.
16. Erlandsson K, Kacperski K, van Gramberg D, Hutton BF. Performance evaluation of D-SPECT: A novel SPECT system for nuclear cardiology. Phys Med Biol 2009;54:2635–49.
17. Dilsizian V, Bacharach SL, Beanlands RS, Bergmann SR, Delbeke D, Gropler RJ, et al. PET myocardial perfusion and metabolism clinical imaging. J Nucl Cardiol 2009;16:651.
18. Sharir T, Slomka PJ, Hayes SW, DiCarli MF, Ziffer JA, Martin WH, et al. Multicenter trial of high-speed versus conventional single-photon emission computed tomography imaging: quantitative results of myocardial perfusion and left ventricular function. J Am Coll Cardiol 2010;55:1965–74.
19. Klocke FJ, Baird MG, Lorell BH, Bateman TM, Messer JV, Berman DS, et al. ACC/AHA/ASNC guidelines for the clinical use of cardiac radionuclide imaging–executive summary: A report of the American College of Cardiology/American Heart Association Task Force on Practice Guidelines (ACC/AHA/ASNC Committee to Revise the 1995 Guidelines for the Clinical Use of Cardiac Radionuclide Imaging). Circulation 2003;108:1404–18.
20. Wang L, Yan C, Zhao S, Fang W. Comparison of (99m)Tc-MIBI SPECT/18F-FDG PET imaging and cardiac magnetic resonance imaging in patients with idiopathic dilated cardiomyopathy: Assessment of cardiac function and myocardial injury. Clin Nucl Med 2012;37:1163–9.
21. Duvall WL, Sweeny JM, Croft LB, Ginsberg E, Guma KA, Henzlova MJ. Reduced stress dose with rapid acquisition CZT SPECT MPI in a non-obese clinical population: Comparison to coronary angiography. J Nucl Cardiol 2012;19:19–27.
22. Duvall WL, Sweeny JM, Croft LB, Barghash MH, Kulkarni NK, Guma KA, et al. Comparison of high efficiency CZT SPECT MPI to coronary angiography. J Nucl Cardiol 2011;18:595–604.
23. Bailliez A, Blaire T, Mouquet F, Legghe R, Etienne B, Legallois D, et al. Segmental and global left ventricular function assessment using gated SPECT with a semiconductor cadmium zinc telluride

(CZT) camera: Phantom study and clinical validation vs cardiac magnetic resonance. J Nucl Cardiol 2014;21:712–22.
24. Einstein AJ, Blankstein R, Andrews H, Fish M, Padgett R, Hayes SW, et al. Comparison of image quality, myocardial perfusion, and left ventricular function between standard imaging and single-injection ultra-low-dose imaging using a high-efficiency SPECT camera: The MILLISIEVERT study. J Nucl Med 2014;55:1430–7.
25. Agostini D, Marie PY, Ben-Haim S, Rouzet F, Songy B, Giordano A, et al. Performance of cardiac cadmium-zinc-telluride gamma camera imaging in coronary artery disease: A review from the cardiovascular committee of the European Association of Nuclear Medicine (EANM). Eur J Nucl Med Mol Imaging 2016;43:2423–32.
26. Giorgetti A, Masci PG, Marras G, Rustamova YK, Gimelli A, Genovesi D, et al. Gated SPECT evaluation of left ventricular function using a CZT camera and a fast low-dose clinical protocol: Comparison to cardiac magnetic resonance imaging. Eur J Nucl Med Mol Imaging 2013;40:1869–75.
27. Cochet H, Bullier E, Gerbaud E, Durieux M, Godbert Y, Lederlin M, et al. Absolute quantification of left ventricular global and regional function at nuclear MPI using ultrafast CZT SPECT: Initial validation versus cardiac MR. J Nucl Med 2013;54:556–63.
28. Abraham WT, Fisher WG, Smith AL, Delurgio DB, Leon AR, Loh E, et al. Cardiac resynchronization in chronic heart failure. N Engl J Med 2002;346:1845–53.
29. Bax JJ, Abraham T, Barold SS, Breithardt OA, Fung JW, Garrigue S, et al. Cardiac resynchronization therapy: Part 1–issues before device implantation. J Am Coll Cardiol 2005;46:2153–67.
30. Kiso K, Imoto A, Nishimura Y, Kanzaki H, Noda T, Kamakura S, et al. Novel algorithm for quantitative assessment of left ventricular dyssynchrony with ECG-gated myocardial perfusion SPECT: useful technique for management of cardiac resynchronization therapy. Ann Nucl Med 2011;25:768–76.
31. Boogers MM, Van Kriekinge SD, Henneman MM, Ypenburg C, Van Bommel RJ, Boersma E, et al. Quantitative gated SPECT-derived phase analysis on gated myocardial perfusion SPECT detects left ventricular dyssynchrony and predicts response to cardiac resynchronization therapy. J Nucl Med 2009;50:718–25.
32. Henneman MM, Chen J, Dibbets-Schneider P, Stokkel MP, Bleeker GB, Ypenburg C, et al. Can LV dyssynchrony as assessed with phase analysis on gated myocardial perfusion SPECT predict response to CRT? J Nucl Med 2007;48:1104–11.